Zoology xxx (2010) xxx–xxx

Contents lists available at ScienceDirect

Zoology

journal homepage: www.elsevier.de/zool

Feeding anatomy, filter-feeding rate, and diet of whale sharks *Rhincodon typus* during surface ram filter feeding off the Yucatan Peninsula, Mexico

Philip J. Motta[a,*], Michael Maslanka[b,1], Robert E. Hueter[c], Ray L. Davis[b,2], Rafael de la Parra[d], Samantha L. Mulvany[a], Maria Laura Habegger[a], James A. Strother[e], Kyle R. Mara[a], Jayne M. Gardiner[a], John P. Tyminski[c,3], Leslie D. Zeigler[b,4]

[a] *Department of Integrative Biology, University of South Florida, 4202 East Fowler Avenue, Tampa, FL 33620, USA*
[b] *Georgia Aquarium, 225 Baker Street, Atlanta, GA 30313, USA*
[c] *Center for Shark Research, Mote Marine Laboratory, 1600 Ken Thompson Parkway, Sarasota, FL 34236, USA*
[d] *Proyecto Domino, Comision Nacional de Areas Naturales Protegidas, P.O. Box 518, Cancun, Quintana Roo, Mexico 77500, Mexico*
[e] *Department of Ecology and Evolution, University of California, Irvine, CA 92697, USA*

ARTICLE INFO

Article history:
Received 5 October 2009
Received in revised form
15 December 2009
Accepted 22 December 2009

Keywords:
Ram filter feeding
Shark diet
Plankton
Feeding rate

ABSTRACT

The feeding anatomy, behavior and diet of the whale shark *Rhincodon typus* were studied off Cabo Catoche, Yucatan Peninsula, Mexico. The filtering apparatus is composed of 20 unique filtering pads that completely occlude the pharyngeal cavity. A reticulated mesh lies on the proximal surface of the pads, with openings averaging 1.2 mm in diameter. Superficial to this, a series of primary and secondary cartilaginous vanes support the pads and direct the water across the primary gill filaments. During surface ram filter feeding, sharks swam at an average velocity of 1.1 m/s with 85% of the open mouth below the water's surface. Sharks on average spent approximately 7.5 h/day feeding at the surface on dense plankton dominated by sergestids, calanoid copepods, chaetognaths and fish larvae. Based on calculated flow speed and underwater mouth area, it was estimated that a whale shark of 443 cm total length (TL) filters 326 m^3/h, and a 622 cm TL shark 614 m^3/h. With an average plankton biomass of 4.5 g/m^3 at the feeding site, the two sizes of sharks on average would ingest 1467 and 2763 g of plankton per hour, and their daily ration would be approximately 14,931 and 28,121 kJ, respectively. These values are consistent with independently derived feeding rations of captive, growing whale sharks in an aquarium. A feeding mechanism utilizing cross-flow filtration of plankton is described, allowing the sharks to ingest plankton that is smaller than the mesh while reducing clogging of the filtering apparatus.

1. Introduction

The whale shark *Rhincodon typus* (Smith, 1828) is the world's largest fish as well as the largest filter feeding fish, yet its feeding biology is still poorly understood. Denison (1937) provided one of the earliest and most thorough descriptions of the head, followed by seminal work by Gudger (1941a,b) who described the shark as having a huge mouth, small teeth and "curious gill arches" composed of sponge-like masses of filtering gill sieves through which the water must pass, and upon which the prey are supposedly trapped before swallowing (Gudger, 1941b, p. 86). The very detailed descriptions of the cranial anatomy by both authors are at odds with the poorly described filtering apparatus. To date Gudger's description remains the most complete description of a unique filtering apparatus found in no other fish. Comparing this filtering apparatus to that of the basking shark *Cetorhinus maximus* and the megamouth shark *Megachasma pelagios*, Taylor et al. (1983) and Sanderson and Wassersug (1993) both concluded that the filtering apparatus of the whale shark is incapable of sustaining a high rate of water flow through it.

Better understood, but still controversial, is the diet of this circumglobal giant. Early scientists recognized that, despite its size, it had a unique filtering apparatus and subsisted on plankton near the surface (Gill, 1905). Gudger (1941a) noted that in addition to planktonic crustaceans, *Rhincodon* had been conclusively demonstrated to feed on squid and cuttlefish. He postulated that an invertebrate diet is insufficient to maintain this species, and summarized observations of whale sharks purportedly ingesting

* Corresponding author. Tel.: +1 813 974 2878; fax: +1 813 974 3263.
E-mail address: motta@usf.edu (P.J. Motta).
[1] Current address: Department of Nutrition, Smithsonian Conservation Biology Institute, Washington, DC 20013, USA.
[2] Current address: Marine Science Center, 100 Lighthouse Drive, Ponce Inlet, FL 32127, USA.
[3] Current address: 14271 Appalachian Trail, Davie, FL 33325, USA.
[4] Current address: Disney's Animal Kingdom, Animal Nutrition Center, Lake Buena Vista, FL 32830, USA.

0944-2006/$ – see front matter © 2010 Elsevier GmbH. All rights reserved.
doi:10.1016/j.zool.2009.12.001

schooling clupeids. Since those early, and often anecdotal, studies, numerous dietary analyses have been conducted at whale shark aggregation sites. These analyses, based on stomach contents, fecal samples, behavioral observations, and plankton tows, indicated that whale sharks primarily feed on a variety of planktonic organisms. These include euphausids, copepods, chaetognaths, crab larvae, molluscs, siphonophores, salps, sergestids, isopods, amphipods, stomatopods, coral spawn, and fish eggs. In addition, they also feed on small squid and fish (Silas and Rajagopalan, 1963; Taylor, 1994, 1996, 2007; Clark and Nelson, 1997; Taylor and Pearce, 1999; Heyman et al., 2001; Wilson and Newbound, 2001; Duffy, 2002; Jarman and Wilson, 2004; Hacohen-Domene et al., 2006; Hoffmayer et al., 2007; Nelson and Eckert, 2007; Meekan et al., 2009).

We now know that whale sharks use at least three methods of filter feeding. The most readily observable, due to its location, is *surface ram filter feeding* or *surface active feeding*. When feeding in this manner, the whale shark swims at the surface with the dorsal surface of the head and usually the dorsal fin and upper lobe of the caudal fin exposed. With its body pitched upwards, the open mouth is held partially out of the water, and the animal swims at relatively slow speeds (0.3–1.5 m/s),[1] ramming the water and food through its filtering apparatus. The shark is occasionally seen to "cough", back-flushing water and particles out of its mouth before resuming feeding (Clark and Nelson, 1997; Heyman et al., 2001; Nelson and Eckert, 2007; Taylor, 2007). During *stationary/vertical suction feeding* the shark either remains relatively horizontal or assumes a nearly vertical position, stops or almost ceases swimming, and actively suctions in plankton or small fish with repeated opening and closing of its mouth. When in the vertical position, the shark's mouth is positioned just below the surface (Gudger, 1941a; Heyman et al., 2001; Nelson and Eckert, 2007). During *sub-surface passive feeding/passive feeding*, the shark swims slowly (0.2–0.5 m/s) (see footnote [1]) below the surface with the mouth wide open, filtering the food from the water (Nelson and Eckert, 2007; Taylor, 2007). Nelson and Eckert (2007) noted that every few minutes the mouth would close and the shark appear to swallow, and no gulping or suction feeding was noted during this behavior. They also observed "coughing" during this feeding behavior.

Despite the growing body of literature on the feeding biology of the whale shark, there is scant detailed information on the anatomy of the filtering apparatus, or the amount and nutrient content of the food ingested. There are no estimates of daily dietary intake, information that is important not only with regards to its basic feeding biology but also its captive husbandry. In this regard we undertook a study of whale shark surface ram filter feeding off the Yucatan Peninsula, Mexico, where one of the largest known aggregations occurs during summer plankton blooms (Hueter et al., 2007). The goals of this study were to: (i) better describe the anatomy of the filtering apparatus; (ii) relate plankton size to filter mesh dimensions; (iii) describe fluid flow into the mouth; (iv) estimate plankton ingestion per unit time during surface ram filter feeding; and (v) estimate nutrient uptake based on ingestion rate and nutrient analysis of the plankton.

2. Materials and methods

2.1. Study area and field methods

Field work was conducted in 2006, 2007, and 2008 on the continental shelf near Isla Holbox and Isla Contoy, north of Cabo Catoche, on the northeastern corner of the Yucatan Peninsula, Mexico. The area sampled ranged from 21°41.545′ to 21°45.811′N and 86°59.898′ to 87°09.866′W, where bottom depth ranged between 10 and 20 m. Between April and September each year at least several hundred whale sharks aggregate in the area to feed on plankton associated with a seasonal upwelling. Population estimates range as high as 1400 sharks visiting the region every summer, with sharks ranging in size from 1.5 to 13 m total length (TL) and a sex ratio of approximately 1 female per 2.6 males (Hueter et al., 2008). Observations were confined to surface ram filter feeding as low underwater visibility (due to dense plankton abundance) mostly prevented sub-surface observations. Observations generally occurred between 07:00 and 14:00 h. Feeding sharks were tracked with a motor vessel at a distance of approximately 2–5 m, taking care not to alter the shark's natural behavior. With the vessel moving at the same rate as, and parallel to, the animal, swimming speed was recorded for 33 sharks with either a Garmin GPS MAP 276C or a Garmin eTrex Venture GPS (Garmin International Inc., Olathe, KA, USA). The swimming speed of each shark was recorded two to three times and an average taken. Swimming speed recorded in this manner closely matched water flow velocity independently recorded by means of calibrated lasers, as described below. Shark TL was estimated to the nearest half-meter for each shark two to three times by motoring within 2–3 m of, and parallel to, the shark and comparing its total length to one-meter markings on the boat gunwale. The average of these length estimates was recorded. In addition, for a subset of these sharks, a pair of calibrated green laser pointers set 50 cm apart were projected on the head, allowing total length to be estimated later from still or video pictures using the ratio of internasal distance or distance of snout to pectoral fin origin, first gill slit, or dorsal fin origin to total length (see Section 2.5).

Above-water video of bubbles or pieces of flotsam was recorded as they entered a shark's open mouth (see electronic supplement, Shark 9 2007 aerial view surface ram filter feeding). In addition, still images were taken of feeding whale sharks from an anterior view, visualizing the exposed portion of the mouth above the water's surface as the animal swam toward the observer. Using the distance measures from the green lasers along with these images, the following data were obtained: percent of open mouth area above the water; absolute mouth width and height (based on internasal width – see Section 2.5) when the laser lights were visible; and velocity of water flow in front of the shark, to compare to swimming speed of the shark as measured by motoring beside the feeding shark. Underwater observations of the shark's mouth while surface ram filter feeding were made by snorkeling within one meter of the head, and lateral images of the feeding sharks were used to calculate the pitch angle. Video images were recorded with either a Sony DCR-TRV 103 or a JVC DVL 9800u digital video camera and still pictures with a Canon A 710IS digital camera, and both video and still images were downloaded to a computer and analyzed field by field with BioMechanica DV-R version 2.4 (BioMechanica, Portland, OR, USA) and SigmaScan Pro software, version 4.01.003 (Systat Software, Inc., San Jose, CA, USA).

2.2. Habitat use

Between May and September from 2006 to 2008, whale shark counts were conducted in the study area for a total of 70 days by either boat or airplane. On only two of these days no whale sharks were seen. Locations of sharks were recorded with a Garmin GPS MAP76 or Garmin GPS V.D. During boat observations each shark was identified by observable characteristics including size, sex, fin shape, spot patterns and other distinctive markings, and was photographed and/or marked by a snorkeler with a conventional external, numbered tag to prevent re-sampling of the same ani-

[1] The swimming velocities in Taylor (2007) are incorrectly printed and should be 0.2–0.5 and 1.0–1.5 m/s for sub-surface passive feeding and surface ram-filter feeding, respectively (personal communication).

Please cite this article in press as: Motta, P.J., et al., Feeding anatomy, filter-feeding rate, and diet of whale sharks *Rhincodon typus* during surface ram filter feeding off the Yucatan Peninsula, Mexico. Zoology (2010), doi:10.1016/j.zool.2009.12.001

mal. Aerial surveys were conducted from a Cessna 207 airplane or ultralight aircraft, flying at 250 m altitude in order to get a 500 m range of visibility on each side of the plane. A total of 689 sharks were observed surface ram filter feeding over 274 h of observation by boat, and 2474 sharks during 72 h of observation by plane. The number of sharks sighted per hour of observation for each hour of the day from 08:00 to 16:00 was compiled for the combined boat and aerial observations. The aerial observations most likely included pseudoreplicated sharks that were counted more than once on different days.

In addition, between 2003 and 2007, a total of 16 whale sharks were tagged with pop-up satellite archival transmitting tags (PAT2, PAT4 and Mk10-PAT versions; Wildlife Computers, Redmond, WA, USA) in the study area, following procedures outlined by Wilson et al. (2006). Each PAT tag was attached to a stainless steel dart (Type SSD, 34 × 8.5 mm; Hallprint Pty. Ltd., Victor Harbor, South Australia) by a 15 cm tether comprising segments of monofilament leader and coated wire. When a surface-swimming shark was spotted and selected for PAT tagging, the research vessel was maneuvered to drop one or two snorkelers off at a position just ahead of the moving shark. Using a pole spear, the tagger inserted the tag's dart through the shark's skin and anchored it several centimeters into the subdermal tissue just below the dorsal fin. The PAT tag archived depth, temperature, and light level measurements at regular intervals (every 30 or 60 s) while attached to the animal for a user-determined duration. After the tag detached from its tether and came to the sea surface, it transmitted summaries of its archived data through the Argos satellite system. Physically recovered PAT tags enabled the retrieval of the full archived data set, providing a detailed profile of the animal's diving behavior. Depth measurements from recovered tags were analyzed to determine the number of minutes spent in surface waters (0–1 m) for each hour of the day. PAT tags had a resolution of ±0.5 m and an accuracy of ±1% of the recorded depth. Only data from when the sharks remained in the study area were utilized in the analysis ($N = 4$). The number of surface minutes for all the recovered tags was combined in a weighted average to estimate the percent of time that the whale sharks spent in surface waters while utilizing the study site.

2.3. Plankton sampling

Plankton samples were taken directly beside, and in some cases in front of, the feeding sharks and subsequently in non-feeding (control) areas at least 1–10 km away from the sharks. A square PVC frame neuston net (0.5 m × 0.5 m, 200 μm; Aquatic Research Instruments, Hope, ID, USA) was used to collect 16 and 23 plankton samples in 2007 and 2008, respectively. A mechanical flowmeter (Model MF315; SeaLite Instruments, Inc., Fort Lauderdale, FL, USA) was used to determine water flow through the mouth of the net during tows. Tows lasted 240 s. Duration of tow, speed of tow, flow meter reading, and GPS coordinates were recorded for each tow.

Immediately after collection, the plankton sample was homogenized in the cod end and two 4 ml subsamples were collected. Each subsample was placed in a light-protected 30 ml plastic (Nalgene) bottle with 18 ml of 10% buffered formalin. The remaining sample was collected in a 500 ml light-protected plastic (Nalgene) bottle and placed on ice for later nutrient analysis. Samples for the determination of nutrient content were frozen for transport once returned to port. Total plankton weight per tow was determined using the sum of frozen samples and preserved subsamples (drained of 10% buffered formalin). Knowing the volume of water filtered by the net for each tow allowed a calculation of plankton weight per cubic liter of seawater.

From the two 4 ml subsamples, plankton were identified and counted according to Johnson and Allen (2005) under an Olympus CX stereo microscope. Prey items were identified to taxa and expressed as a percent count of total composition. Extrapolating to the complete sample, the number of plankters per cubic liter of seawater was calculated. In addition, plankton size was measured from 50 random individuals from each of the 39 subsamples (total 1950 plankters measured). Random sampling was ensured by marking the sorting dish into subsections and using a random number generator to pick which subsections, and subsequently plankters, to sample. Length and width were taken for most of the plankters except for shrimp where depth replaced width. All measurements were performed with a Wild M5 stereo microscope and reticle. Measuring criteria varied among species. For shrimp, length was taken from the base of the eyes to the tip of the telson, and depth was taken at the posterior region of the cephalothorax. For copepods, amphipods and chaetognaths, length was taken from the most anterior to the most posterior portion of the body. Setae, antennae or other types of flexible structures were not accounted for in these measurements. Lastly, for fish eggs, the diameter was measured.

2.4. Nutrient analysis

A subsample of plankton (preserved frozen) was used to determine nutrient content (carried out by NP Aanalytical Laboratories, St. Louis, MO, USA; and by Omaha's Henry Doorly Zoo, Omaha, NE, USA). Total dry matter was measured using a forced air oven at 105 or 133 °C (AOAC, 1984). Total fat was determined using a hexane extraction process (AOAC, 1984), protein was determined using a Leco nitrogen/protein determinator (model FP-2000; Leco Corporation, St. Joseph, MI, USA) (AOAC, 1995), ash was determined using a muffle furnace (500–550 °C, AOAC, 1984), and fatty acid profiles were determined using gas chromatography (model 5880; Hewlett-Packard, Palo Alto, CA, USA). Gross energy was determined by calculation (Church and Pond, 1988).

2.5. Anatomical measures

Four whale sharks (shark A, male, TL[2] ~622 cm; shark B, male, TL (see footnote [2]) ~593 cm; shark C, female, TL ~443 cm; and shark D, female, TL ~482 cm) acquired off Hualien, Taiwan and housed at the Georgia Aquarium, Atlanta, were used for morphological measures in addition to a fifth male captive whale shark at the Georgia Aquarium (TL 486 cm) and incomplete but published measurements for 17 whale sharks (TL 394–975 cm) (Smith, 1829, 1849; Haly, 1883; Thurston, 1894; Bean, 1905; Gudger, 1915; Mowbray, 1923; Gudger and Mowbray, 1930; Gudger, 1931; Silas and Rajagopalan, 1963; Bass et al., 1975; Uchida, 1990). Open mouth width-to-height ratio was also measured from five additional underwater photographs of feeding whale sharks (size not determined). Morphometrics included: TL; distance from snout to first dorsal fin, first gill slit and origin of pectoral fin; open mouth width and height; internasal distance; and dorsal fin height. The two male captive sharks (A and B) were anesthetized with 125 mg/l of MS222 (tricaine methanesulphonate), and while restrained in a submerged pen their mouths were opened maximally and dimensions were taken with a tape measure. The two female specimens (C and D) were restrained without anesthesia and measurements were taken. From the above measurements various ratios of each measure to total length were calculated and means taken, as well as ratios of landmarks such as open mouth width and height to internasal distance. From these ratios we were able to calculate the average percent mouth area above the water from the video and still pictures, validate the approximate total lengths of field-observed sharks measured with

[2] These are average estimated total lengths as the measurements taken live and at necropsy (sharks A and B) differ slightly.

Please cite this article in press as: Motta, P.J., et al., Feeding anatomy, filter-feeding rate, and diet of whale sharks *Rhincodon typus* during surface ram filter feeding off the Yucatan Peninsula, Mexico. Zoology (2010), doi:10.1016/j.zool.2009.12.001

the calibrated lasers, and calculate open mouth area from underwater frontal pictures of feeding sharks.

After two of the male specimens died for reasons unrelated to this study (shark A, June 2007; shark B, January 2007), necropsies were performed, including a partial dissection of the filtering apparatus. The complete pharyngeal filtering apparatus was removed from one side, as well as portions from the opposite side. In cases where an upper or lower filtering pad was missing from one side, the equivalent pad from the other side was used for measurement. Digital pictures of the filtering pads were taken of the freshly dead specimens and the area of each filtering pad was measured with SigmaScan Pro software. The tissue was subsequently stored frozen and thawed for the following measures. Of the 21 available of 40 total pads (10 from shark A, 11 from shark B), nine 1 cm^2 sampling areas per pad were recorded with digital macro photography and mesh[3] diameter was measured. The mesh possesses an irregular geometry so the mesh diameter was measured at the shortest or widest regions of 50 openings selected haphazardly from each sampling area, totaling 9450 diameter measures (Table 1 and Fig. 1). All measurements were averaged to estimate mean mesh diameter per pad and for all pads combined. For each of the nine sub-sampled areas per pad an open area ratio β was calculated. Open area ratio is the open area per unit area of pad. The mean β for each pad was then calculated by averaging the ratio for all of the nine sampled areas, and an overall β was calculated for all available pads for each shark. When multiplied by the combined total area of all filtering pads, the total area through which water can potentially flow is expressed, providing the openings are not blocked by plankton or other material. The height and spacing of the primary and secondary vanes (Fig. 1) on the undersurface of each available pad was measured with a digital caliper at three equidistant midline locations for each of the pads (24 measurements for shark A and 36 for shark B). To estimate the dimensions of the outflow respiratory channel distal to the filtering pads, the distances between the primary lamellae (width of the channel) were measured between the third and fourth holobranch on shark A (the only pair still intact). The height of the channel was taken as the length of the underside of the upper plus lower filtering pads on arches I to IV, and the channel depth was the distance from the edge of the secondary vanes to the distal edge of the primary filaments on arches I and III. Digital images were analyzed with SigmaScan Pro software.

2.6. Fluid flow through the filtering apparatus

The volume of water entering the mouth was calculated using a simple hydrodynamic model of flow through the respiratory tract. Fluid particles were assumed to be negligibly affected by viscous forces as they passed into the buccal cavity of the animal (the Reynolds number based on mouth diameter and swimming speed is $\sim 5 \times 10^5$). Thus, the pressure within the buccal cavity was estimated using Bernoulli's equation:

$$p_m = \frac{1}{2}\rho(U_s^2 - U_m^2), \quad (1)$$

where p_m is the pressure in the buccal cavity, ρ is the density of seawater, U_s is the swimming speed of the animal, and U_m is the flow velocity at the mouth. Conversely, the flow through the filtering pad was assumed to be laminar and subject to relatively large viscous forces (the Reynolds number based on the mesh diameter and the flow velocity at the pad given $U_m = U_s$ is $\sim 3 \times 10^2$). The pressure across the filtering pad was then calculated by estimating the

[3] The term mesh is used instead of pore when describing the holes in the filtering pads as they are irregular in shape.

Table 1
Morphometric measurements from the filtering pads of two male whale sharks, both left and right sides combined.

		Upper pads					Lower pads					Upper total area	Lower total area	Mean
		U1	U2	U3	U4	U5	L1	L2	L3	L4	L5			
Shark A (622 cm TL)	Area (cm^2)	1058.44	1001.74	991.16	1002.10	1180.32	1100.54	1066.92	1040.58	1006.68	1349.98	5233.76	5564.70	
	β	0.46	0.50	0.48	0.44	0.47	0.44	0.47	0.49	0.49	0.32			0.46
	Mesh diameter (cm)	0.11	0.10	0.10	0.09	0.08	0.08	0.09	0.10	0.10	0.09			0.09
Shark B (593 cm TL)	Area (cm^2)	1130.81	1274.95	1028.87	1015.53	1004.30[a]	1065.05[a]	1311.58	1110.83	1218.31	1647.20	5454.46	6352.97	
	β	0.61	0.59	0.61	0.54	–	0.57	0.54	0.69	0.58	–			0.60
	Mesh diameter (cm)	0.17	0.15	0.14	0.12	–	0.14	0.15	0.14	0.12	–			0.14

Area values for shark A were duplicated for unavailable contralateral pads.
[a] Area partially extrapolated from non-damaged contralateral pad; dashes denote absent pads.

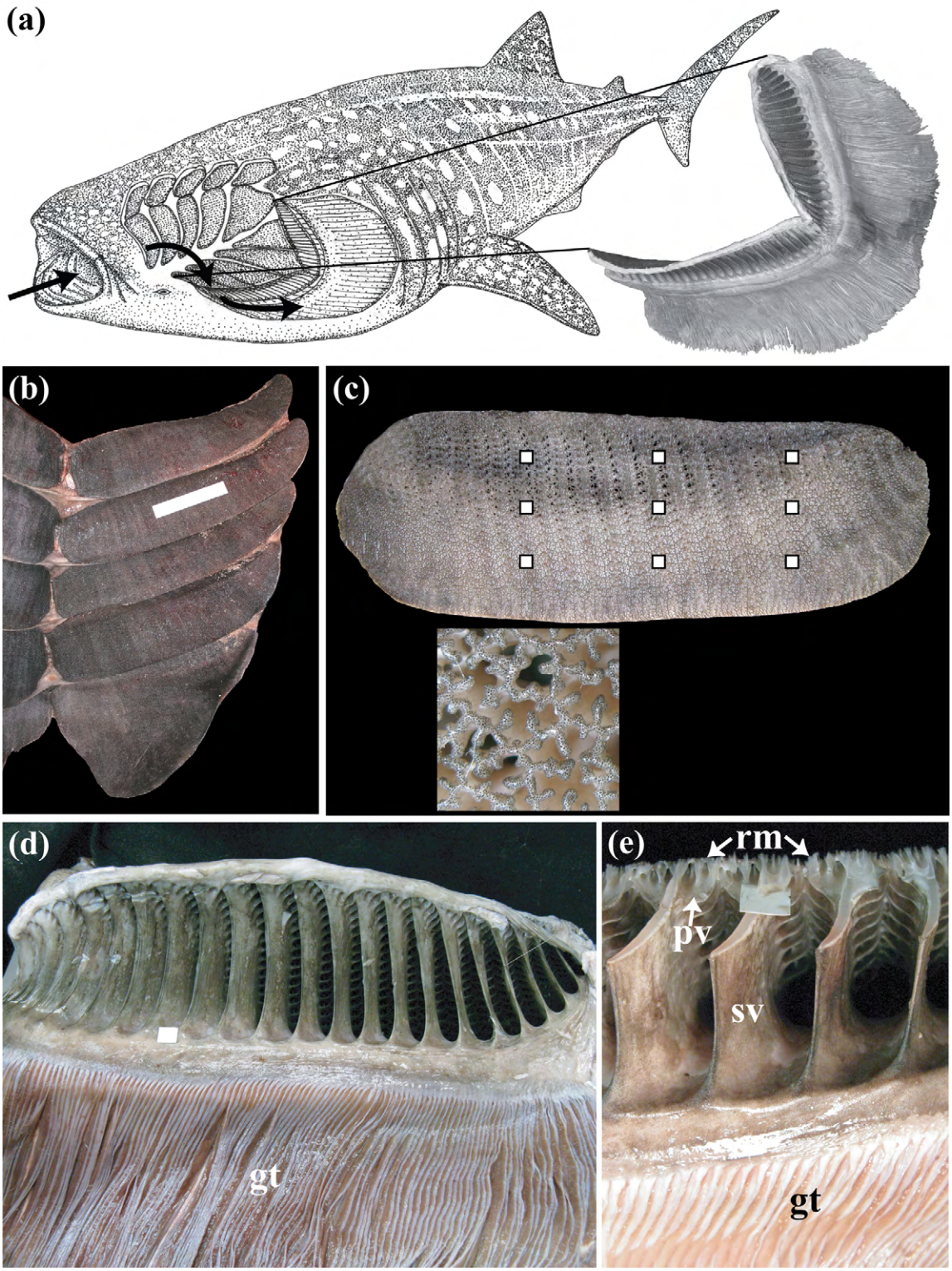

Fig. 1. (a) Schematic representation of a surface ram filter feeding whale shark, showing the approximate position of the filtering pads and the direction of water flow through them. Detail drawing shows a lateral view of the vanes deep to the filtering mesh, as well as the primary gill filaments on the first branchial arch over which the water flows. (This illustration is, with permission, based upon a copyrighted illustration by Emily S. Damstra.) (b) Gross morphology of the whale shark filtering pads. Dorsal view of the lower filtering pads of shark A. The most posterior lower pad at the bottom is triangular in shape, and the lateral side of the pads is to the left. The lateral raphe between the lower and upper pads is visible toward the left. All other soft tissue has been removed. White ruler is 15 cm. (c) The upper second filtering pad of shark B. Because it is an upper pad, lateral is to the left and posterior toward the top. Upper pads are not as falcate on their medial margin as the lower pads. The squares (1 cm × 1 cm) indicate areas sampled to measure mesh diameter, and the detail is a representative square area showing the irregularly shaped holes of the reticulated mesh. (d) External view of the first upper left pad of shark A with lateral margin toward the left. Note that the secondary vanes direct water laterally into the parabranchial chamber and over the gill tissue (gt) before it exits the pharyngeal slit (not shown). White square is 1 cm × 1 cm in size. (e) Close-up of a section through the third left lower filtering pad of shark A showing the reticulated mesh (rm), primary vanes (pv), secondary vanes (sv), and gill tissue (gt). Water flow is through the mesh, between the primary and secondary vanes, and over the gill tissue. White square is 1 cm.

Please cite this article in press as: Motta, P.J., et al., Feeding anatomy, filter-feeding rate, and diet of whale sharks *Rhincodon typus* during surface ram filter feeding off the Yucatan Peninsula, Mexico. Zoology (2010), doi:10.1016/j.zool.2009.12.001

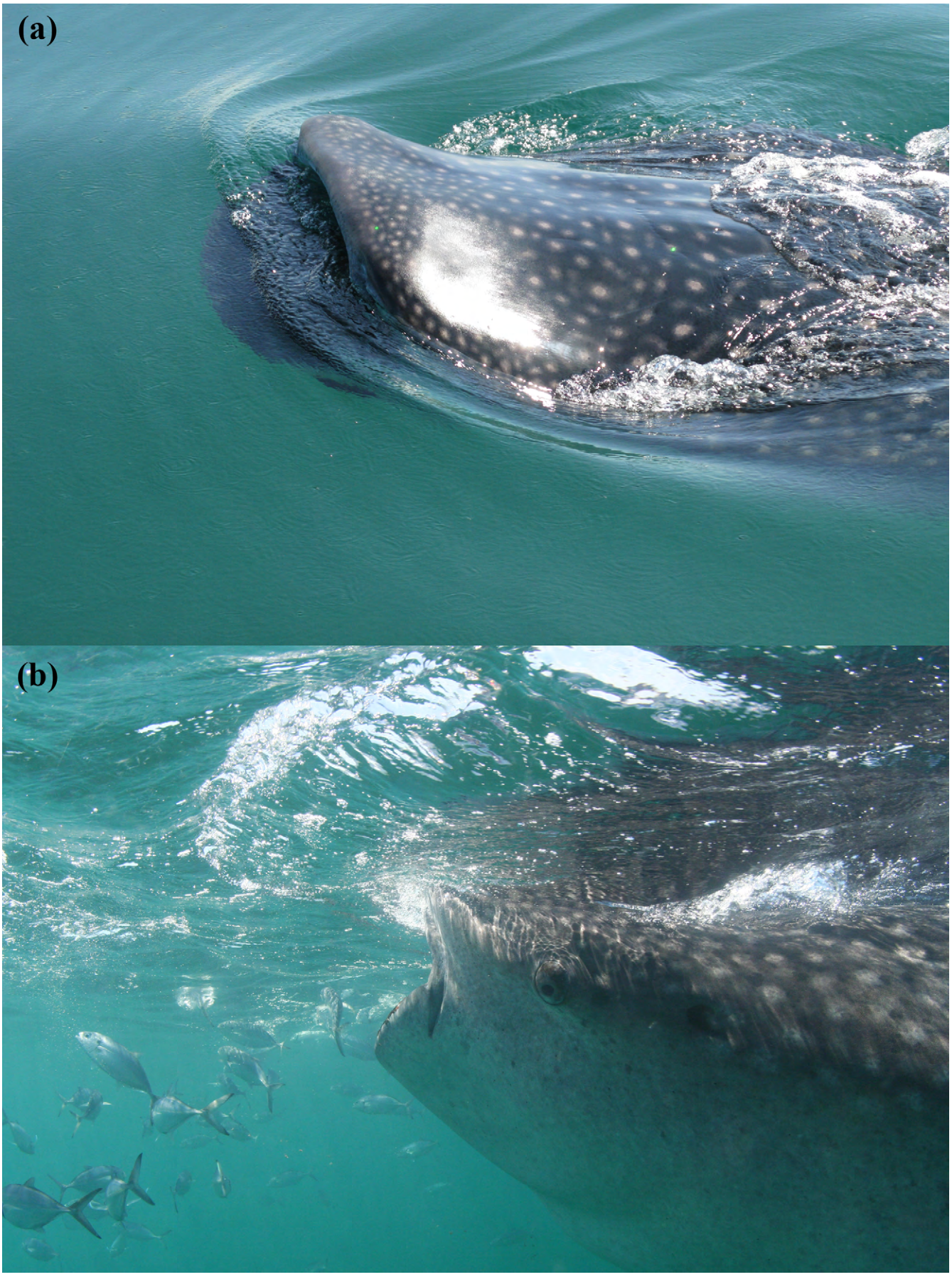

Fig. 2. Surface (a) and sub-surface (b) view of two surface ram filter feeding whale sharks (size between 5 and 8 m TL). Note that the majority of the open mouth is underwater and a bow wave is formed by the lateral edges of the mouth.

Please cite this article in press as: Motta, P.J., et al., Feeding anatomy, filter-feeding rate, and diet of whale sharks *Rhincodon typus* during surface ram filter feeding off the Yucatan Peninsula, Mexico. Zoology (2010), doi:10.1016/j.zool.2009.12.001

hydraulic resistance of the mesh entrance and the mesh length:

$$p_m - p_e = \Delta p_s(U_m) + \Delta p_p(U_m), \quad (2)$$

where p_e is the pressure downstream of the filtering pad, and $\Delta p_s(U_m)$ and $\Delta p_p(U_m)$ are the pressure drops at the mesh entrance and across the mesh length, respectively, as a function of the flow velocity at the mouth. The pressure drop at the mesh entrance, Δp_s, from losses associated with the constriction of the flow as it enters the mesh, was calculated from an empirical model of flow passing into a regularly spaced grid of openings (Idelchik, 1986). This model incorporates the effects of the mesh's Reynolds number, hydraulic diameter, and open area ratio. The pressure drop across the mesh length, Δp_p, was calculated from an analytical model of the flow at the entrance of a cylindrical tube (Fargie and Martin, 1971). This model differs from the commonly used Hagen–Poiseuille equation in that it accounts for the increasing boundary layer thickness within the entrance region of the tube, which makes it consistent with both experimental and numerical studies of flow in the entrance region (Ward-Smith, 1980). Lastly, it was assumed that the hydraulic resistance downstream of the filtering pad was negligible and that fluid at the gill openings remained at ambient pressure, such that the downstream pressure, p_e, was also equal to ambient pressure. Mouth and mesh dimensions were taken as the average of the measured morphologies, mesh holes were assumed to be circular, and the fluid density and viscosity were that of seawater at 25.5 °C (Dietrich et al., 1980). This model makes use of a number of simplifying assumptions regarding the mesh morphology. The sensitivity of the calculated mouth velocity to these assumptions was examined by varying mesh parameters within a realistic range; the resulting range in predicted mouth velocity is presented in Section 3.4. Eqs. (1) and (2) were solved for the flow velocity at the mouth, U_m, using a numerical root-finding algorithm (MATLAB 7.6.0; Mathworks, Inc., Natick, MA, USA).

2.7. Statistics

Plankton lengths and widths between feeding and non-feeding areas were compared by Mann–Whitney rank sum test due to the very unbalanced sample sizes. Amphipod and crab measures were not tested due to small sample size. Plankton densities between feeding and non-feeding (control) sites were compared by a two-tailed t test after ln transformation, and similarly, plankton biomass after square root transformation. Swimming speed of the feeding animals was related to total length with a linear regression. Nutrient data, being very unbalanced with only 2 samples at non-feeding areas and 24 at feeding areas, were tested with a Mann–Whitney rank sum test. All tests were conducted with an alpha level of 0.05 and tests were performed with SigmaStat version 3.1 (SSI, San Jose, CA, USA).

The experiments and observations conducted during this research comply with the Animal Care and Use Committee of the University of South Florida protocol numbers W 3170 and W 2255; the knowledge and permission of the Comision Nacional de Areas Naturales Protegidas (CONANP) of the Secretaria de Medio Ambiente y Recursos Naturales (SEMARNAT), Mexico; and the requirements of the Georgia Aquarium Conservation, Research and Animal Care Committee.

3. Results

3.1. Field observations

In 2006, 2007 and 2008, a total of 33 whale sharks ranging in size from 450 to 850 cm TL were tracked by boat while surface ram filter feeding north of Cabo Catoche. The average water temperature was 25.5 °C and average swimming speed during this feeding behavior was 1.1 ± 0.04 m/s (mean ± s.e.m.); range 0.5–1.6 m/s). Swimming speed was not related to total length ($F = 0.201$, df = 1, $p = 0.657$). The sharks ($N = 20$) swam at an average angle of ~13 ± 0.3° upward pitch with their heads at or slightly above the water surface such that the dorsal surface of their head and part or all of the dorsum between the rostrum and the first dorsal fin was exposed (see electronic supplement Shark 11 2006 underwater view of surface ram filter feeding). Underwater and surface observations during surface ram filter feeding indicated that the open mouth formed an ellipse with the internal width greater than the height. During the surface ram filter feeding, an average of 15.3 ± 1.0% ($N = 27$, 105 measures) of the vertical height of the open mouth was above the water's surface; however, many sharks surface fed with the open mouth completely underwater with only the dorsum of the head and anterior body above water. When visible, the laser calibration indicated flow rate in front of the shark matched swim speed of the shark as measured by GPS. Flow around the lateral edges of the mouth (formed by the labial cartilages) formed a bow wave such that water medial to each bow wave entered the mouth (Fig. 2; see also electronic supplements Shark 6 2008 aerial view of surface ram filter feeding and Shark 9 2007 aerial view of surface ram filter feeding). Coughing during surface ram filter feeding, resulting in material being forcefully expelled out of the mouth, was observed on numerous occasions (see electronic supplement Shark 8 2008 coughing behavior). Time between coughs ranged from 3.25 to 13 min (mean = 7.4 min, ±1.6 s.e.m., $N = 5$). Vertical suction feeding was not observed.

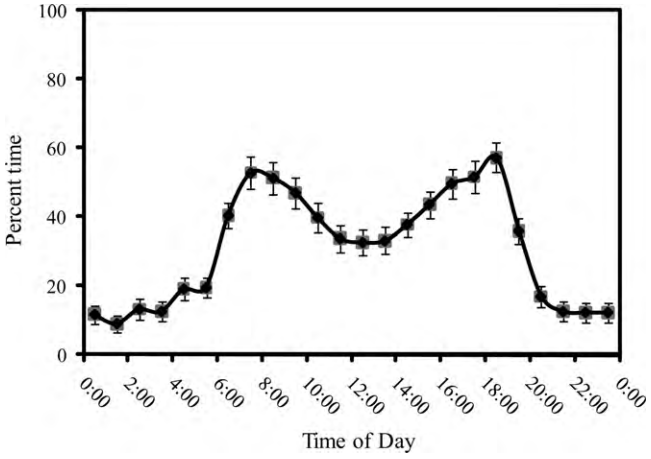

Fig. 3. Hourly percent time spent in surface waters (0–1 m) by satellite tagged whale sharks in the study area. The reported percentages are weighted averages of four sharks representing 67 days of archival depth data. Standard error bars for the four sharks are indicated by hour. Overall, the four sharks spent an average of 31.1% or 7.5 h/day in surface waters.

Four deployed PAT tags were physically recovered from whale sharks tagged at the study site, comprising three males (5.5–7 m TL) and one female (7 m TL). The archived surface depth data (0–1 m depth range) were only analyzed for the periods of 1, 2, 18, and 46 days after tagging, respectively, for a combined total of 67 days of data where the sharks remained in the study area. Expressing these combined data as an hourly weighted average revealed a pattern of greater surface swimming in the morning (06:00–10:59, 46.3%), a decrease around mid-day (11:00–13:59, 33.2%), followed by increased surface swimming in the mid- to late afternoon (14:00–18:59, 48.0%), and the least surface swimming at night (19:00–05:59 = 16.0%) (Fig. 3). Overall, these sharks spent on average 31.1% of the time, equal to 7.5 h/day, in surface waters.

Combined aerial and boat counts indicated a pattern similar to the satellite-tagged sharks with the number of sharks per hour of observation peaking during mid-morning, the sharks retreat-

Please cite this article in press as: Motta, P.J., et al., Feeding anatomy, filter-feeding rate, and diet of whale sharks *Rhincodon typus* during surface ram filter feeding off the Yucatan Peninsula, Mexico. Zoology (2010), doi:10.1016/j.zool.2009.12.001

Table 2
Combined length and width (mm) data of plankters in feeding and non-feeding areas.

2007 + 2008	Feeding area			Non-feeding area		
	Length (mm)	Width (mm)	*N*	Length (mm)	Width (mm)	*N*
Sergestids	10.38[a]	0.66[a]	842	9.72	0.60	187
Chaetognaths	10.74	0.69[a]	237	10.73	0.62	72
Copepods	1.07[a]	0.34[a]	188	0.86	0.26	239
Fish eggs	1.03	1.03	13	0.94	0.94	133
Crabs	2.28	1.14	7	1.59	1.11	2
Amphipods	0.82	0.34	2	0.57	0.15	2

N is the number of plankters measured in each category; for sergestids depth replaces width; crabs include both zoea and megalopae.
[a] Significantly greater in feeding sites.

ing to sub-surface waters about noon, and again increasing slightly in number at the surface in mid-afternoon (Fig. 4). The few boat observations of sub-surface swimming, obscured by low underwater visibility, indicated some sharks were using sub-surface passive feeding while the majority swam with their mouths mostly closed.

3.2. Plankton composition, size and nutrient analysis

In the feeding areas, plankton was dominated by sergestid shrimp (57.2%), calanoid copepods (15.9%), chaetognaths (12.8%), and fish larvae (12.2%). In non-feeding areas, plankton was dominated by calanoid copepods (45.4%), fish larvae (20.8%), sergestid shrimp (15.9%), and chaetognaths (12.1%).

In 2007 and 2008, the median length of plankters in the feeding areas ranged from 0.82 to 10.74 mm, and width from 0.34 to 1.14 mm. In the non-feeding areas the length ranged from 0.57 to 10.73 mm, and the width ranged from 0.15 to 0.94 mm. The three dominant prey items, sergestids, copepods, and chaetognaths, were greater in width at feeding sites compared to non-feeding sites for the two years combined ($t = 80337.500$, $p < 0.001$; $t = 44595.500$, $p < 0.001$; $t = 9217.000$, $p = 0.003$, respectively), and sergestids and copepods were greater in length ($t = 76888.000$, $p < 0.001$; $t = 44742.000$, $p < 0.001$) (Table 2).

Nutrient content (protein, lipid, ash, kJ) as well as moisture did not differ between feeding and non-feeding areas ($p = 0.163$–0.885), but this result must be viewed with caution as only 2 samples at non-feeding sites were compared to samples at 24 feeding sites. Moisture content of plankton samples from feeding areas was $88.9 \pm 0.46\%$, mean crude protein content was $6.3 \pm 0.32\%$ (as a percent of total wet weight), mean lipid content was $0.8 \pm 0.05\%$, and mean ash content was $3.5 \pm 0.10\%$. Mean calculated gross energy of the plankton was 1.357 ± 0.084 kJ/g (wet weight) or 12.225 kJ/g dry weight.[4]

Mean plankton density was greater (1841 ± 616 per m^3) in the feeding areas than in the non-feeding (control) areas (752 ± 429 per m^3; $t = -2.171$, 32 df, $p = 0.037$). Likewise, plankton biomass was about 2.5 times greater at feeding sites (4.5 ± 0.6 g/m^3 wet weight) than at non-feeding sites (1.8 ± 0.7 g/m^3 wet weight; $t = 3.232$, 32 df, $p = 0.003$).

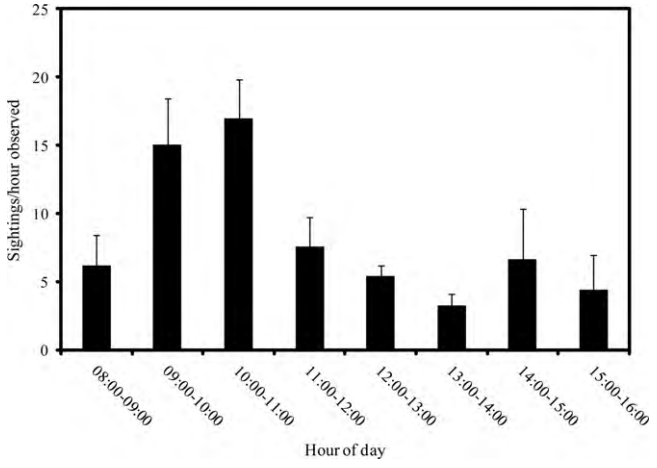

Fig. 4. Number of sightings of sharks surface ram filter feeding per unit hour of observation from 08:00 to 16:00 h, based on combined boat and aerial observations of 3163 sightings over 346 h of observation from 2006 to 2008. Standard errors are indicated.

3.3. Anatomy

Anatomical measurements indicated maximum internal mouth width was 12.0% ($N = 8$), and mouth height 6.3% ($N = 10$) of TL, and the open mouth width to height ratio was 1.9 ($N = 10$). Internasal width was 10.0% of TL ($N = 11$), and vertical mouth height/internasal width was 0.61 ($N = 11$). Based on open mouth internal heights, the estimated total open mouth area was 2035 cm^2 for shark A (622 cm TL), 1841 cm^2 for shark B (593 cm TL), and 1079 cm^2 for shark C (443 cm TL) ($N = 4$ frontal pictures of feeding sharks).

The anterior margin of the mouth is funnel-shaped with the labial cartilages forming the lateral walls of the funnel. Mouth width, as recorded here, refers to the narrowest aperture of the funnel, in essence the anterior dimensions of a "tube" through which water may flow.[5] Posterior to the upper and lower bands of tiny teeth are two upper and two lower passive buccal valves. In the 593 cm TL male shark, the anterior lower buccal valve was 3 cm wide, and attached by a frenulum at the midline, and the posterior lower valve was 10 cm wide and also was attached at the midline. The anterior upper valve was 3 cm and the posterior upper valve was 4 cm wide and neither was attached at the midline.

On each side of the pharynx there are five lower and five upper filtering pads. The lower pads were larger in area than the corresponding upper pads (Table 1). The most posterior pads were the largest. The first four pads were approximately rectangular in shape, whereas the fifth pads were somewhat triangular with their apex pointed posteriorly (Fig. 1). Adjacent pads from anterior to posterior were jointed by a flexible raphe of connective tissue. A similar raphe also ran medially, joining the right and left pads dorsally and ventrally. This tissue was connected to the pharyngeal wall anteriorly and to the entrance of the esophagus posteriorly, such that water must pass through the pads to exit to the parabranchial chamber and eventually out through the pharyngeal clefts. The entire pharyngeal basket is therefore flexible and can collapse or expand, particularly in the sagittal plane. The cartilaginous branchial arches I–IV were lateral to and between the filtering pads I–V and their raphes.

[4] Total dry weight, not ash-free dry weight.
[5] Consequently, other authors either refer to mouth width as the widest part of the funnel or the narrow aperture, without clearly explaining which measure they are taking.

Please cite this article in press as: Motta, P.J., et al., Feeding anatomy, filter-feeding rate, and diet of whale sharks *Rhincodon typus* during surface ram filter feeding off the Yucatan Peninsula, Mexico. Zoology (2010), doi:10.1016/j.zool.2009.12.001

The pharyngeal surface of each filtering pad was composed of a denticle-covered reticulated mesh with irregularly shaped holes. Superficial to this mesh were uniformly arranged cartilaginous primary vanes which merged to form a series of larger cartilaginous secondary vanes, which in turn opened into the parabranchial cavity (Fig. 1). These secondary vanes, the "ladder-rung partitions" of Gudger (1941b, p. 94), spanned the branchial arches and supported the filtering pad laterally. Water must therefore flow through the mesh, between the primary and secondary vanes, and over the primary gill filaments of four holobranchs which lay between adjacent pads, lateral to the cartilaginous branchial arches. A hemibranch was located on the anterior surface of the first pharyngeal cleft. The fifth and most posterior pads were supported externally by greatly flattened cartilaginous pharyngobranchials (upper) and ceratobranchials (lower). Water flowing through the posterior end of the fifth triangular filtering pad is directed anteriorly by these flattened cartilages and a connective tissue floor. It must flow over the most posterior hemibranch and into the parabranchial chamber before exiting through the pharyngeal clefts.

The total area of the filtering pad for shark A and B was estimated at 10,799 and 11,807 cm^2, respectively, with an average area of 11,303 cm^2. Average mesh diameter was 0.9 mm for shark A and 1.4 mm for shark B, with a mean of 1.2 ± 0.1 mm (Table 1). Some of the filtering pads of shark B were superficially abraded during necropsy, perhaps leading to the slightly larger diameter. The open area ratio β was 0.46 ± 0.02 for shark A and 0.60 ± 0.02 for B, with a mean of 0.52 ± 0.02 for both sharks. The average height and width of the primary vanes for both sharks was 12.0 ± 0.2 and 5.2 ± 0.1 mm, respectively, and the average combined height of the primary and secondary vanes was 33.6 ± 0.5 mm (Fig. 1). The average distance between the spacing of the secondary vanes was 16.9 ± 1.6 mm. The ratio of combined height (primary + secondary vanes) to width (primary vanes) was 6.5. The excurrent parabranchial channel of shark A had a width of ~6 cm, a dorso-ventral height of ~80 cm, and a streamwise depth of ~20 cm.

3.4. Filtering volume and energetics

The hydrodynamical model presented above indicated that the flow velocity of water entering the mouth was nearly equal to the swimming speed and was relatively constant over a realistic range of parameter values. For the measured morphology, the flow velocity at the mouth was calculated to be 90.4% of the swimming speed. The sensitivity of these calculations was assessed by independently varying the mesh diameter (0.9–1.5 mm), mesh length (5–15 mm), and mesh opening shape (elliptical or rectangular geometry, with a fineness ratio that varied between 1.0 and 5.0). Such calculations produced a range of mouth velocities between 86.1% and 93.5% of the swimming speed.

Given the measured morphology and the calculated flow velocity at the mouth, it was possible to calculate the Reynolds number for each element of the flow tract. Using the mouth width and the mean flow velocity through the mouth, the Reynolds number at the mouth opening was estimated to be 7.3×10^5 for a whale shark swimming at 1.1 m/s. Using the mesh opening diameter and the mean flow velocity through each mesh opening, the Reynolds number within the mesh was estimated to be 3.0×10^2. Using the half-width of the parabranchial chamber and the mean flow velocity through this channel, the Reynolds number within the outflow of the filtering apparatus was estimated as 1.0×10^4. Additionally, the hydrodynamical model was used to calculate the pressure head across the filtering apparatus, which was estimated to be 113 Pa for a whale shark swimming at 1.1 m/s.

The biomass ingested was estimated by calculating the volume of water passing through the partially submerged mouth per unit time multiplied by the mean biomass of plankton per unit volume. With an average of 84.7% of the open mouth underwater during surface ram filter feeding, a 443 cm TL shark would present an open mouth area of ~914 cm^2 (84.7% of 1079) and a 622 cm TL shark an open mouth area of ~1724 cm^2 (84.7% of 2035) to the water. With a flow velocity at the mouth of 0.99 m/s (90.4% of 1.1 m/s) the smaller shark would filter 0.0914 $m^2 \times 0.99$ m/s or 0.0905 m^3/s of water = 326 m^3/h, and the larger shark would filter 614 m^3/h. With an average plankton biomass of 4.5 g/m^3 at the feeding sites, the sharks would, on average, ingest 1467 and 2763 g of plankton per hour, respectively, and for an average feeding time of 7.5 h per day, a total of 11,003 and 20,723 g of plankton/day, which at 1.357 kJ/g equates to 14,931 and 28,121 kJ per day, respectively.

4. Discussion

4.1. Feeding behavior

The aggregation of juvenile and adult male and female whale sharks off the Yucatan Peninsula is among the most important population centers for the species and is the largest whale shark aggregation site known in the world (Hueter et al., 2008). During the course of this study the sharks spent the majority of daylight hours in the summer months surface ram filter feeding or swimming just below the surface in the shallow, plankton-rich waters north of Cabo Catoche. This aggregation of sharks appears to occur in response to upwelling currents off the eastern Campeche Bank, which bring nutrient-rich waters that produce abundant plankton (Merino, 1997; Pérez et al., 1999; Zavala-Hidalgo et al., 2006; Cardenas-Palomo, 2007). The plankton tends to concentrate at or just below the surface, particularly before 11:30–12:00 h each day during the summer months (de la Parra, personal observation). Similar aggregations in response to plankton blooms or mass spawning events also occur at: Ningaloo Reef, Australia (Colman, 1997; Wilson et al., 2001; Taylor, 2007); Gulf of Tadjoura, Djibouti (Rowat et al., 2007); off the Seychelles, Mozambique, and Maldives (Rowat and Gore, 2007); Gladden Spit, Belize (Heyman et al., 2001); the Galapagos Islands (Arnbom and Papastavrou, 1988); the Gulf of California (Clark and Nelson, 1997; Hacohen-Domene et al., 2006; Nelson and Eckert, 2007); and the northern Gulf of Mexico (Hoffmayer et al., 2007).

The behavior of whale sharks swimming with the body inclined upward and the open mouth partially or totally submerged is consistent with the reports from other localities where plankton-rich surface waters occur (Clark and Nelson, 1997; Heyman et al., 2001; Nelson and Eckert, 2007; Taylor, 2007). The swimming speeds observed during this type of feeding ranged from 0.5 to 1.6 m/s (average 1.03 m/s) and are remarkably similar to speeds of surface feeding whale sharks in the north central Gulf of Mexico (average speed 1.03 m/s; Hoffmayer et al., 2007), off Baja California (0.3–1.1 m/s; Nelson and Eckert, 2007) and Ningaloo Reef, Australia (1.0–1.5 m/s; Taylor, 2007). This average swimming speed for 29 sharks of average TL 6.7 m is slightly less than the predicted optimum swimming speed (1.13 m/s) for energy conservation for swimming fish ($U_0 = 0.503L^{0.43}$; Weihs, 1977; Weihs et al., 1981). The latter theoretical predictions are, however, based on smaller bony fishes and would be an overestimate for larger sharks with lower maintenance costs (Weihs, personal communication), although the estimates have been shown to be very accurate for 2 m standard length *Carcharhinus leucas* and *C. plumbeus* (Weihs et al., 1981). Eckert and Stewart (2001) also found that whale sharks had occasional travel rates of 1.1 m/s but when traversing longer distances averaged 0.3 m/s. Rowat and Gore (2007) similarly found ground speeds between 0.3 and 0.7 m/s for whale sharks traversing long distances. However, these long distance averages include periods of vertical movement including deep

Please cite this article in press as: Motta, P.J., et al., Feeding anatomy, filter-feeding rate, and diet of whale sharks *Rhincodon typus* during surface ram filter feeding off the Yucatan Peninsula, Mexico. Zoology (2010), doi:10.1016/j.zool.2009.12.001

dives (Eckert and Stewart, 2001; Graham et al., 2006; Wilson, 2006; Wilson et al., 2006; Brunnschweiler et al., 2009), and time and distance required to execute dives is generally not considered in these swimming speed calculations. Thus, whale sharks may make horizontal oceanic crossings at higher speeds than localized movements suggest (Rowat and Gore, 2007). The average swimming speed for filter feeding basking sharks (4–6.5 m TL) is 0.85 m/s (range 0.76–0.94 m/s), which is 29–39% slower than the speed predicted by the model of Weihs and Webb (1983) (Sims, 2000b). As was suggested for basking sharks, we expect that swimming with an open mouth and swimming at the surface increases drag on whale sharks, effectively reducing the optimum swimming speed (Videler, 1993; Sims, 2000b). While the pressure at the mouth opening is reduced by the flow of water into the buccal cavity, the pressure head over the mesh imparts a drag force onto the filtering apparatus. It would seem likely that the total drag is increased both by the passage of water through the small mesh openings as well as by any flow separation that may occur as a result of the outflow from the gill openings. This is consistent with studies of filter feeding bony fishes, in which filter feeding animals have a metabolic rate elevated above that of non-feeding animals even beyond that which would be expected simply from differences in swimming speed (James and Probyn, 1989; Macy et al., 1999). On the other hand, a lower than expected swimming rate may represent the most efficient speed for filtering plankton through the unique filtering pads. Although not recorded, it appeared that surface ram filter feeding whale sharks at the Yucatan Peninsula site reduced their swimming speed when encountering a particularly dense plankton patch, as do whale sharks feeding on fish spawn off Belize (Heyman et al., 2001) and plankton-feeding basking sharks (Sims, 1999). The whale shark body pitch of approximately 13° most likely permits lift generation by the ventral body surface and pectoral fins at these relatively low speeds (Wilga and Lauder, 2000), allowing the sharks to keep their open mouths at the water's surface.

Our satellite tags and observational data both indicate that whale sharks off Cabo Catoche approach the surface to filter feed during the early morning, peak in abundance during mid-morning, return to slightly deeper waters around noon, and resurface to feed in the afternoon, returning to deeper waters again in the late afternoon. Although on-water observations were not made at night, satellite tag data indicate limited surface activity during night hours. In almost all cases, when the sharks were swimming between 0 and 1 m depth in the daytime they were surface ram filter feeding at the study site. When the sharks retreated to slightly deeper waters (~2–6 m) and were still visible from the surface, they were often swimming with their mouths slightly open and apparently not filter feeding. These diurnal vertical movements are most likely related to diel vertical migrations of the plankton. Time spent at the surface by basking sharks depends largely on the minimum abundance of prey in the surface layer and time of day and is timed to plankton migration, and lower, near threshold, levels of zooplankton abundance may be more important in determining surface duration than higher levels (Sims et al., 2003, 2005). Our satellite tag estimate of four whale sharks spending on average 7.5 h/day within 0–1 m depth, presumably feeding at the surface, is in close agreement with Rowat and Gore (2007) and Rowat et al. (2009), who found from pop-up archival tags that whale sharks off the Seychelles spent on average 60% of daylight hours (7.2 h/day) within 10 m of the surface. In the Gulf of California (Sea of Cortez), whale sharks spend more than or equal to 80% of their time (24 h) at depths less than 10 m; however, the satellite tracking method used to determine this was admittedly biased towards shallower depths (Eckert and Stewart, 2001). In the western Indian Ocean, two tagged whale sharks spent on average 7.8 h/day at the surface (shark 1 = 5.6 h/day, shark 2 = 10.0 h/day at surface) and an average of 13.9 h/day between 0 and 5 m depth (Brunnschweiler et al., 2009, personal communication). These accounts, however, do not differentiate between feeding and non-feeding behavior.

4.2. Diet and foraging behavior

The surface ram filter feeding whale sharks observed off the Yucatan Peninsula sought out surface aggregations of plankton dominated by sergestid shrimp, calanoid copepods, chaetognaths, and fish larvae. The three dominant prey items (sergestids, copepods and chaetognaths) were greater in width at feeding sites compared to non-feeding sites, and shrimp and copepods were greater in length. The sharks were often observed to turn repeatedly to stay within the denser plankton patches, which were visibly reddish in color. Off La Paz, Mexico, whale sharks have been observed suction feeding in dense patches of plankton, primarily copepods, and they stayed in the patches with frequent turns (Clark and Nelson, 1997). At Bahía de Los Angeles, Baja California, whale sharks also fed on dense plankton patches primarily composed of copepods, but interestingly varied feeding method with plankton density (Nelson and Eckert, 2007). Surface ram filter feeding occurred at a mean plankton density of 86.9×10^3 m^{-3}, which was over 4 times greater than densities observed during vertical suction feeding, and 14 times greater than during sub-surface passive feeding. Our recorded mean plankton density off the Yucatan Peninsula was much lower (1841 ± 616 per m^3), and even lower than densities recorded during the sub-surface feeding by sharks off Baja California (5900 per m^3) (Nelson and Eckert, 2007). In the northern Gulf of Mexico, whale sharks surface ram filter feed on eggs of little tunny *Euthynnus alletteratus* at densities of 9000 eggs per m^3 (Hoffmayer et al., 2007). Our relatively low densities could be in part due to the plankton being primarily confined to the very surface waters whereas the plankton net sampled to a depth of approximately 45 cm.

4.3. Anatomy, prey and mesh diameter

The whale shark's filtering pads are a unique autapomorphic character. Although their homology is unclear, Denison (1937), Gudger (1941b) and Compagno (1984) referred to them as gill rakers. During filter feeding, water enters the elliptical mouth, passes into the pharynx, proceeds through the 20 filtering pads exiting between the primary and secondary vanes, passes over the primary gill filaments and into the parabranchial chamber, and exits the external gill slits. The flexible raphe joining the filtering pads laterally and mid-sagittally prevents water discharge anywhere but through the filtering pads and allows the pharyngeal cavity to expand in the sagittal plane. The large labial cartilages laterally occlude the mouth opening, directing water into the funnel-shaped oral cavity, and the passive buccal valves help to prevent the backflow of water when the mouth is closed. Similar labial cartilages and buccal valves are found in the orectolobid suction feeding nurse shark *Ginglymostoma cirratum* (Motta and Wilga, 1999). When observed inside the pharyngeal cavity of an actively feeding whale shark, the upper filtering pads are more horizontal in orientation than the ventral pads, which tend to be ventrally displaced and presented to the incoming water at an acute angle due to the ventrally bulging pharyngeal cavity (Figs. 1 and 5).

During surface ram filter feeding we observed little or no evidence of pulsatile suction feeding. This is in agreement with observations by Taylor (2007). The gill slits remained open and gently fluttering as the animals swam forward and there was no indication of rhythmical pumping as has been seen during stationary/vertical suction feeding and in some cases sub-surface passive feeding (Clark and Nelson, 1997; Heyman et al., 2001). On one occasion, when a shark encountered what appeared to be a particularly dense plankton patch the shark slowed to a near stop

Please cite this article in press as: Motta, P.J., et al., Feeding anatomy, filter-feeding rate, and diet of whale sharks *Rhincodon typus* during surface ram filter feeding off the Yucatan Peninsula, Mexico. Zoology (2010), doi:10.1016/j.zool.2009.12.001

Fig. 5. Anterolateral view into the pharynx of an actively feeding whale shark showing the angle of the lower pads relative to open mouth. The branchiohyoid apparatus can depress ventrally, thereby enlarging the cavity and orienting the lower pads, in particular, so that they face the incoming water at an acute angle.

and commenced pulsatile suction feeding while remaining at the usual swimming angle, with the dorsal surface of the head and body above the water's surface.

Total filtering area of the pads greatly exceeds the open mouth area, which is expected to reduce the flow resistance incurred by the filtering pads. The estimated total open mouth area was 2035 cm^2 for shark A (622 cm TL), and 1841 cm^2 for shark B (593 cm TL). Even during surface ram filter feeding, in which an average of 84.7% of the open mouth was underwater, the area through which water passes into the buccal cavity (~1724 and 1559 cm^2, respectively) was notably smaller than the total filtering pad area in both sharks (10,799 cm^2 and 11,807 cm^2, respectively). However, the total filtering pad area includes both the area of the mesh openings and the area of the mesh itself. The ratio of the area of the openings to the total area, the open area ratio β, was 0.46 for shark A and 0.60 for shark B. Accounting for this, the open area through which water can pass through the filtering pads was 4924 and 7096 cm^2 for sharks A and B, respectively. As the pads become clogged with plankton, the effective mesh diameter would decrease as the total open area, leading to the "coughing" behavior that back-flushes the pads and clears them (Hoffmayer et al., 2007; Nelson and Eckert, 2007; Taylor, 2007; this study).

4.4. Filtering mechanism

Consideration of the filter feeding mechanism in whale sharks has focused on two potential methods: *dead-end sieving* and *hydrosol filtration* (Gudger, 1941a,b; Clark and Nelson, 1997). In dead-end sieving, water and the entrained particles approach approximately perpendicular to the filter and particles larger than the pores are trapped while smaller particles pass through. Conversely, in a hydrosol filter, the filtering surfaces have some adhesive properties, possibly as a result of being covered with sticky mucus, such that any particle that contacts a filtering element sticks to it and is captured. The particles encounter the hydrosol filter due to hydrodynamic processes such as direct interception and inertial impaction, allowing particles even smaller than the pores to be retained (Rubenstein and Koehl, 1977; LaBarbera, 1984). However, recent work on filter feeding in bony fishes has implicated a third potential filtering mechanism known as *cross-flow filtration*. In this method, the water and entrained particles pass approximately parallel to the gill arches or filter pads while traveling at high velocities. As the suspension travels posteriorly, the water exits between the gill rakers or through the filtering pads, and the particles are concentrated into a bolus at the rear of the pharynx where they can be swallowed (Brainerd, 2001; Sanderson et al., 2001; Callan and Sanderson, 2003; Cheer et al., 2006). This mechanism results in the entrapment of both larger and smaller particles, reduces fouling of the filtering apparatus, concentrates particles in the posterior pharyngeal cavity, and transports the food to the entrance of the esophagus. It has been demonstrated to function during suspension feeding in some bony fishes (Sanderson et al., 2001; Callan and Sanderson, 2003; Smith and Sanderson, 2007) and has been hypothesized to contribute to filter feeding in fin whales (Goldbogen et al., 2007). Cross-flow filtration is also used in numerous industrial applications, particularly where it is necessary to reduce clogging of the filter element (Ripperger and Altmann, 2002).

The hydrodynamics of filter feeding in whale sharks appear to be comparable to that observed in filter feeding bony fishes and baleen whales. The Reynolds number for flow through a single mesh opening of the filtering apparatus was estimated to be ~300. This is within the range of 150–600 observed for flow past the gill rakers of suspension feeding bony fishes (Sanderson et al., 2001) and is comparable to the value of 570 reported for flow past the baleen fringes of fin whales (Goldbogen et al., 2007). At such a Reynolds number, flow through the channel is expected to remain laminar even for ducts with rough surfaces (Ward-Smith, 1980). The pressure drop across the mesh was calculated to be 113 Pa for a whale shark swimming at 1.1 m/s. This relatively small pressure head is consistent with the absence of a large bow wave, as was observed in videos of surface feeding whale sharks. Interestingly, this differential is markedly less than the ~2000 Pa pressure head that was calculated for bowhead whales during continuous filter feeding (for a 10 m body length swimming at 1.1 m/s; Werth, 2004). It is unclear whether this disparity arises from morphological differences or differences in how the flow through the respiratory tract was modeled. However, the pressure head of 113 Pa calculated for whale sharks is consistent with the pressure observed across fish gills during routine ventilation, which falls between 30 and 200 Pa for a diverse range of taxa (Hughes, 1960a,b; Burggren and Bemis, 1992; Ferry-Graham, 1999).

Several workers have questioned the effectiveness of the whale shark's filtering pads at sustaining a high flow of water through them during ram filter feeding (Taylor et al., 1983; Sanderson and Wassersug, 1993) and their ability to filter out plankton smaller than the holes in the filtering pads (Clark and Nelson, 1997). Although the majority of plankters ingested by the whale sharks off Cabo Catoche are greater in length than the average mesh diameter of the filter pads (1.2 mm), the ability to feed on plankton less than the diameter of the openings in the filter pads enhances the food resources available to the whale shark. At Gladden Spit in Belize, the sharks were observed feeding in areas dominated by fish eggs of 0.75–0.78 mm diameter (Heyman et al., 2001) and in the northern Gulf of Mexico whale sharks surface ram filter feed in water abundant with fish eggs of 0.70–0.80 mm diameter (Hoffmayer et al., 2007). If whale sharks relied on dead-end sieving to perform filter feeding, the majority of such plankton would likely not be captured. However, if whale sharks are able to utilize either hydrosol filtration or cross-flow filtration, then it is possible that such items could be effectively retained. There is no direct evidence for cross-flow filtration in whale sharks, but the morphology suggests this may be an important mechanism in their filter feeding. The filtering pads of the whale shark, particularly the lower pads, lie at an acute angle to the incoming water when the mouth is open and the pharynx distended, such that the bulk of the water flow

Please cite this article in press as: Motta, P.J., et al., Feeding anatomy, filter-feeding rate, and diet of whale sharks *Rhincodon typus* during surface ram filter feeding off the Yucatan Peninsula, Mexico. Zoology (2010), doi:10.1016/j.zool.2009.12.001

might be expected to be parallel or near parallel to the filtering pads (Figs. 1 and 5). Additionally, in computational models of filter feeding in bony fishes, vortices were observed near the esophageal opening (Cheer et al., 2001). If such vortices exist in whale sharks, they could act to increase the flow velocities parallel to the filtering pads. As a feeding mechanism in whale sharks, cross-flow filtration is an intriguing hypothesis in part because it might explain how the sharks are able to feed on very dense aggregations of plankton and not quickly clog their filter pads. In three species of bony fishes using cross-flow filtration only a very small amount of the ingested particles contacted the filtering apparatus and accumulated there (Sanderson et al., 2001). Such a mechanism would explain how whale sharks ingest large volumes of plankton yet "cough" relatively infrequently to clear the filtering pads. By comparison, filter feeding bowhead whales (*Balaena mysticetus*) pause to clean the baleen about every 2.5 min (Simon et al., 2009). Such coughs by whale sharks may perform a role similar to the temporary reversals of flow within the oropharyngeal cavity of some bony fishes, which lift and clear mucus and particles from the branchial arches (Smith and Sanderson, 2008).

The consequences of the filtering pads and primary and secondary vanes for the excurrent flow also remain unclear. The effect of flow passing through mesh-like bodies has been studied to the greatest extent in the context of water and wind tunnel design. In the construction of wind tunnels, thin screens are used to produce a uniform flow across a section by imposing a uniform, static pressure drop. However, while the screens improve uniformity they also produce small-scale turbulence. It has been observed that screens with an open area ratio β greater than 0.57 reduce this production of excess turbulence (Mehta and Bradshaw, 1979). Thick collimators are used to dissipate upstream vortices larger than the cell diameter by restricting the lateral velocities. However, while they dissipate vortices larger than the cell diameter, collimators will also produce vortices that are smaller than the cell diameter. Thus, collimators are most effective at reducing the total turbulence when the cell length is approximately 6–8 times the cell diameter (Mehta and Bradshaw, 1979). Interestingly, the filtering pad has an open area ratio of 0.53 while the vanes form "cells" with a combined height (primary + secondary vanes) to width (primary vanes) ratio of 6.5. While the geometry of the filtering pads is certain to be constrained by their role in filtering plankton, it is possible that it also serves to "condition" the outflow. The Reynolds number of the excurrent channels was estimated to be $\sim 10^4$. At these Reynolds numbers the flow is very likely turbulent, but the nature of that turbulence is uncertain. In the initial length of a parallel channel, such as the parabranchial chamber, the flow is characterized by high-frequency, small-scale turbulence and reduced boundary layer thickness (Byrne et al., 1969). However, after this initial length, the flow is dominated by low-frequency, large-scale turbulence and the boundary layer extends the entire channel width (Clark, 1968; Moin and Kim, 1985). It is possible that the primary and secondary vanes act to reduce the upstream turbulence in the parabranchial chamber and delay the formation of low-frequency vortices within the relatively short outflow tract (~4 channel widths long). Reduction of such turbulence within the outflow tract may be important in reducing the hydrodynamic losses that would otherwise increase backpressure and reduce the flow of water through the filtering pad.

4.5. Energetics

The whale, basking, and megamouth sharks are among the largest fishes and all are planktivores. As such they must filter large volumes of water and consume large quantities of prey for maintenance and growth. A surface ram filter feeding whale shark of 4.4 m is estimated to filter 326 m^3/h, and a 6.2 m shark 614 m^3/h. In comparison, 5 m basking sharks are calculated to filter 432 m^3/h during sub-surface ram filter feeding (Sims, 1999). The estimated daily ration of 14,931 kJ for a 443 cm TL whale shark and 28,121 kJ for a 622 cm TL whale shark are the first *in situ* estimates for the species. These are probably conservative estimates when considering that sharks at other localities may feed in much higher plankton densities (Hoffmayer et al., 2007; Nelson and Eckert, 2007). However, a similarly analyzed and independently derived daily ration for captive and growing whale sharks (515–664 cm TL) at the Georgia Aquarium is 17,287–31,238 kJ/day) (Zeigler, personal observation). The similarity in daily ration for these sharks is surprising considering metabolic differences due to captivity, temperature and other environmental factors (Cortes and Gruber, 1994; Schmid and Murru, 1994; Carlson et al., 2004). In contrast, an 8.4 m TL whale shark at the Okinawa Churaumi Aquarium is fed a daily ration of 50,242–83,736 kJ/day (S. Uchida and K. Sato, pers. comm.). Unfortunately, lacking length–weight data for these whale sharks, direct comparison of daily ration to other elasmobranchs, which is usually expressed as a proportion of mean body weight per day, is impossible (Wetherbee and Cortes, 2004). These caloric estimates must be taken with caution because of possible errors that could include an underestimate of the number of hours feeding per day, not accounting for sub-surface feeding which could contribute to the former, and variance and errors in calculating mouth area from digital photographs of sharks with their mouths apparently fully open. Taylor (2007) observed whale sharks with their mouths approximately 50% open when surface ram filter feeding; however, during our underwater observations these surface-feeding sharks appeared to have their mouths fully open the majority of the time. In addition, plankton counts will vary by site and time, and energy per gram will vary with plankton composition (Davis, 1993).

In contrast to whale and megamouth sharks, which can use suction and ram feeding to collect plankton, basking sharks rely solely on forward swimming to ram filter feed their prey (Taylor et al., 1983; Compagno, 1990; Sims, 2000a; Nakaya et al., 2008). As such, for basking sharks that only ram filter feed and incur high drag from the open mouth, there is a threshold prey density estimated at approximately 0.62 g wet weight/m^3, below which the animals should cease feeding because net energy gain can no longer be achieved (Sims and Quayle, 1998; Sims, 1999, 2000a). Off Plymouth, UK, basking sharks forage in areas with zooplankton densities ranging from 0.47 to 8.29 g wet weight/m^3, and when density was below the background level of 0.50–0.80 g/m^3, the sharks ceased feeding (Sims, 1999). This predicted foraging threshold for basking sharks is much lower than the plankton density observed at the whale shark feeding sites off the Yucatan Peninsula (4.5 ± 0.6 g/m^3) and even lower than at non-feeding sites (1.8 ± 0.7 g/m^3). By contrast, basking sharks in Monterey Bay, California, off the Pacific coast of Vancouver Island, Gulf of Maine, and north of Santa Cruz Island, California select plankton patches (primarily copepods) with densities ranging from 739 to 2647 plankters/m^3, very similar to our recorded average density of 1841 per m^3 (Baduini, 1995). The latter plankton biomass was recorded in a region of upwelling and high plankton density and during surface ram filter feeding, which is reported to occur at the highest plankton densities (Nelson and Eckert, 2007). Missing in our data are plankton densities for feeding areas not characterized by upwelling and plankton blooms, values which would be instructive in gaining a better understanding of overall energetic costs for the whale shark. Nevertheless, we hypothesize that whale sharks, similar to basking sharks (Sims and Merrett, 1997; Sims and Quayle, 1998; Sims, 1999), may avoid feeding at an energetic loss by moving within ocean basins to forage in high productivity regions. This leads to patchiness in whale shark distribution and potentially an erosion of population structure, heightening the need to manage conservation plans for these

Please cite this article in press as: Motta, P.J., et al., Feeding anatomy, filter-feeding rate, and diet of whale sharks *Rhincodon typus* during surface ram filter feeding off the Yucatan Peninsula, Mexico. Zoology (2010), doi:10.1016/j.zool.2009.12.001

magnificent animals on a global scale (Taylor, 1996; Eckert and Stewart, 2001; Eckert et al., 2002; Castro et al., 2007; Schmidt et al., 2009).

4.6. Future directions

Utilizing fluid models, fluid flow through the filtering pads and the putative cross-flow filtration mechanism should be investigated. Further estimates of daily ration would provide insight into the energetics of the world's largest fish and augment captive husbandry. Future studies should also investigate nutritional requirements and feeding on a longer time and area scale, spanning not only these regions of rich plankton biomass but also other feeding sites. We must also consider the possibility of feeding, prey choice and energetics during deep dives of whale sharks, which have been recorded to depths of more than 1700 m and ambient temperatures of about 4 °C (Tyminski et al., 2008). Lastly, it would be instructive to determine if diel vertical migrations of the whale shark, even on such a small scale as occurs off Cabo Catoche, is related to vertical movements of its plankton food base.

Acknowledgements

We sincerely thank Jeronimo Aviles and Eugenio Aceves for providing photographs of whale sharks, Juerg Brunnschweiler for providing us his satellite tag data on two whale sharks, and Lisa Whitenack for help with whale shark dissections. This project was supported by generous contributions from: the Georgia Aquarium; Proyecto Domino, Comision Nacional de Areas Naturales Protegidas, Mexico; NOAA/NMFS to the National Shark Research Consortium; Mote Marine Laboratory; University of South Florida; the Porter Family Foundation; and an additional anonymous foundation. We sincerely thank Jaime Gonzalez, Paco Remolina, and Montserrat Trigo for their unrelenting support and encouragement. Emily Damstra generously allowed us to base our illustration of the feeding whale shark on her marvelous original illustration (www.emilydamstra.com).

Appendix A. Supplementary data

Supplementary data associated with this article can be found, in the online version, at doi:10.1016/j.zool.2009.12.001.

References

AOAC, 1984. Official Methods of Analysis, 14th edition. Association of Official Analytical Chemists, Washington, DC.
AOAC, 1995. Official Methods of Analysis, 15th edition. Association of Official Analytical Chemists, Washington, DC.
Arnbom, T., Papastavrou, V., 1988. Fish in association with whale sharks *Rhincodon typus* near the Galápagos Islands. Notic. Galápagos 46, 3–15.
Baduini, C.L., 1995. Feeding ecology of basking sharks (*Cetorhinus maximus*) relative to distribution and abundance of prey. M.S. Thesis, Moss Landing Marine Laboratories, San Jose State University, San Jose.
Bass, A.J., D'Aubrey, J.D., Kistnasamy, N., 1975. Sharks of the east coast of southern Africa. IV. The families Odontaspididae, Scapanorhynchidae, Isuridae, Cetorhinidae, Alopiidae, Orectolobidae and Rhiniodontidae. S. Afr. Assoc. Mar. Biol. Res., Oceanogr. Res. Inst., Invest. Rep., 39.
Bean, B.A., 1905. The history of the whale shark (*Rhinodon typicus* Smith). Smiths. Misc. Coll. 48, 139–148.
Brainerd, E.L., 2001. Caught in the crossflow. Nature 412, 387–388.
Brunnschweiler, J.M., Baensch, H., Pierce, S.J., Sims, D.W., 2009. Deep-diving behaviour of a whale shark *Rhincodon typus* during long-distance movement in the western Indian Ocean. J. Fish Biol. 74, 706–714.
Burggren, W.W., Bemis, W.E., 1992. Metabolism and ram gill ventilation in juvenile paddlefish, *Polyodon spathula* (Chondrostei: Polyodontidae). Physiol. Zool. 65, 515–539.
Byrne, J., Hatton, A.P., Marriott, P.G., 1969. Turbulent flow and heat transfer in the entrance region of a parallel wall passage. Proc. Instn. Mech. Engrs. 184, 697–712.
Callan, W.T., Sanderson, S.L., 2003. Feeding mechanisms in carp: crossflow filtration, palatal protrusions and flow reversals. J. Exp. Biol. 206, 883–892.
Cardenas-Palomo, N., 2007. Distribucion espacio-temporal de variables hidrobiologicas asociadas con el uso del habitat del tiburon ballena (*Rhinocodon typus*) en el noreste de la peninsula de Yucatan. Tesis de Maestría, Instituto Politécnico Nacional, Merida, Mexico.
Carlson, J.K., Goldman, K.J., Lowe, C.G., 2004. Metabolism, energetic demand, and endothermy. In: Carrier, J.C., Musick, J.A., Heithaus, M.R. (Eds.), Biology of Sharks and Their Relatives. CRC Press, Boca Raton, pp. 203–224.
Castro, A.L.F., Stewart, B.S., Wilson, S.G., Hueter, R.E., Meekan, M.G., Motta, P.J., Bowen, B.W., Karl, S.A., 2007. Population genetic structure of the Earth's largest fish, the whale shark (*Rhincodon typus*). Mol. Ecol. 16, 5183–5192.
Cheer, A.Y., Ogami, Y., Sanderson, S.L., 2001. Computational fluid dynamics in the oral cavity of ram suspension-feeding fishes. J. Theor. Biol. 210, 463–474.
Cheer, A.Y., Cheung, S., Sanderson, S.L., 2006. Computational fluid dynamics 2004. In: Proceedings of the Third International Conference on Computational Fluid Dynamics, ICCFD3, Toronto, 12–16 July 2004, In: Groth, C., Zingg, D.W. (Eds.), Computational Fluid Dynamics of Crossflow Filtration in Suspension-Feeding Fishes. Springer, Berlin Heidelberg, pp. 301–306.
Church, D.C., Pond, W.G., 1988. Basic Animal Feeding and Nutrition. John Wiley and Sons, New York.
Clark, E., Nelson, D.R., 1997. Young whale sharks, *Rhincodon typus*, feeding on a copepod bloom near La Paz, Mexico. Environ. Biol. Fishes 50, 63–73.
Clark, J.A., 1968. A study of incompressible turbulent boundary layers in channel flow. Trans. ASME J. Basic Eng. 90, 455–468.
Colman, J.G., 1997. A review of the biology and ecology of the whale shark. J. Fish Biol. 51, 1219–1234.
Compagno, L.J.V., 1984. FAO Species Catalogue. Vol. 4. Sharks of the World. Part 1. Hexanchiformes to Lamniformes. FAO Fisheries Synopsis 125, Vol. 4, Part 1. Food and Agriculture Organization of the United Nations, Rome.
Compagno, L.J.V., 1990. Relationships of the megamouth shark *Megachasma pelagios* (Lamniformes: Megachasmidae), with comments on its feeding habits. In: Pratt, H.L.J., Gruber, S.H., Tamiuchi, T. (Eds.), Elasmobranchs as a Living Resource: Advances in the Biology, Ecology, Systematics, and the Status of the Fisheries, vol. 90. National Marine Fisheries Service, pp. 357–379.
Cortes, E., Gruber, S.H., 1994. Effect of ration size on growth and gross conversion efficiency of young lemon sharks, *Negaprion brevirostris*. J. Fish Biol. 44, 331–341.
Davis, N.D., 1993. Caloric Content of Oceanic Zooplankton and Fishes for Studies of Salmonid Food Habits and Their Ecologically Related Species (NPAFC Doc.) FRI-UW-9312. Fisheries Research Institute, University of Washington, Seattle.
Denison, R.H., 1937. Anatomy of the head and pelvic fin of the whale shark *Rhineodon*. Bull. Am. Mus. Nat. Hist. 73, 477–515.
Dietrich, G., Kalle, K., Krauss, W., Siedler, G., 1980. General Oceanography. John Wiley & Sons, Inc., New York.
Duffy, J.C.A., 2002. Distribution, seasonality, lengths, and feeding behaviour of whale sharks (*Rhincodon typus*) observed in New Zealand waters. N. Z. J. Mar. Freshw. Res. 36, 565–570.
Eckert, S.A., Stewart, B.S., 2001. Telemetry and satellite tracking of whale sharks, *Rhincodon typus*, in the Sea of Cortez, Mexico, and the northern Pacific Ocean. Environ. Biol. Fishes 60, 299–308.
Eckert, S.A., Dolar, L.L., Kooyman, G.L., Perrin, W., Rahman, A., 2002. Movements of whale sharks (*Rhincodon typus*) in South-east Asian waters as determined by satellite telemetry. J. Zool. London 257, 111–115.
Fargie, D., Martin, B.W., 1971. Developing laminar flow in a pipe of circular cross-section. Proc. R. Soc. A 321, 461–476.
Ferry-Graham, L.A., 1999. Mechanics of ventilation in swellsharks, *Cephaloscyllium ventriosum* (Scyliorhinidae). J. Exp. Biol. 202, 1501–1510.
Gill, T., 1905. On the habits of the great whale shark (*Rhineodon typus*). Science 21, 790–791.
Goldbogen, J.A., Pyenson, N.D., Shadwick, R.E., 2007. Big gulps require high drag for fin whale lunge feeding. Mar. Ecol. Prog. Ser. 349, 289–301.
Graham, R.T., Roberts, C.M., Smart, J.C.R., 2006. Diving behaviour of whale sharks in relation to a predictable food pulse. J. Royal Soc. Interface 3, 109–116.
Gudger, E.W., 1915. Natural history of the whale shark, *Rhineodon typus* Smith. Zoologica 1, 345–389.
Gudger, E.W., 1931. The fourth Florida whale shark, *Rhineodon typus*, and the American Museum model based on it. Bull. Am. Mus. Nat. Hist. 61, 613–637.
Gudger, E.W., 1941a. The food and feeding habits of the whale shark *Rhineodon typus*. J. Elisha Mitchell Sci. Soc. 57, 57–72.
Gudger, E.W., 1941b. The feeding organs of the whale shark, *Rhineodon typus*. J. Morphol. 68, 81–99.
Gudger, E.W., Mowbray, L.L., 1930. Whale shark! How a specimen of the greatest of living sharks, *Rhineodon typus*, was captured near Marathon, Florida; and how it was towed near Key West. Nat. Hist. 30, 182–192.
Hacohen-Domene, A., Galvan-Magana, F., Ketchum-Mejia, J., 2006. Abundance of whale shark (*Rhincodon typus*) preferred prey species in the southern Gulf of California, Mexico. Cybium 30, 99–102.
Haly, A., 1883. On the occurrence of *Rhincodon typicus* Smith on the west coast of Ceylon. Ann. Mag. Nat. Hist. Ser. 5, 48–49.
Heyman, W.D., Graham, R.T., Kjerfve, B., Johannes, R.E., 2001. Whale sharks *Rhincodon typus* aggregate to feed on fish spawn in Belize. Mar. Ecol. Prog. Ser. 215, 275–282.
Hoffmayer, E.R., Franks, J.S., Driggers III, W.B., Oswald, K.J., Quattro, J.M., 2007. Observations of a feeding aggregation of whale sharks, *Rhincodon typus*, in the north central Gulf of Mexico. Gulf Caribb. Res. 19, 1–5.
Hueter, R., Gonzalez Cano, J., De la Parra, R., Tyminski, J., Perez-Ramirez, J., Remolina-Suarez, F., 2007. Biological studies of large feeding aggregations of whale sharks (*Rhincodon typus*) in the southern Gulf of Mexico. In: Irvine, T.R., Keesing, J.K.

(Eds.), The First International Whale Shark Conference: Promoting International Collaboration in Whale Shark Conservation, Science and Management. Conference Overview, Abstracts and Supplementary Proceedings. CSIRO Marine and Atmospheric Research, Australia.
Hueter, R.E., Tyminski, J.P., de la Parra, R., 2008. The geographical movements of whale sharks tagged with pop-up archival satellite tags off Quintana Roo, Mexico. In: Proceedings of the 2nd International Whale Shark Conference, Holbox, Quintana Roo, Mexico, 15–20 July 2008, Available at: http://www.domino.conanp.gob.mx/doc_conf/Bob.pdf.
Hughes, G.M., 1960a. The mechanism of gill ventilation in the dogfish and skate. J. Exp. Biol. 37, 11–27.
Hughes, G.M., 1960b. The mechanism of gill ventilation in marine teleosts. J. Exp. Biol. 37, 28–45.
Idelchik, I.E., 1986. Handbook of Hydraulic Resistance. Hemisphere Publishing, New York.
James, A.G., Probyn, T., 1989. The relationship between respiration rate, swimming speed and feeding behaviour in the Cape anchovy *Engraulis capensis* Gilchrist. J. Exp. Mar. Biol. Ecol. 131, 81–100.
Jarman, S.N., Wilson, S.G., 2004. DNA-based species identification of krill consumed by whale sharks. J. Fish Biol. 65, 586–591.
Johnson, W.S., Allen, D.M., 2005. Zooplankton of the Atlantic and Gulf Coasts: A Guide to Their Identification and Ecology. Johns Hopkins University Press, Baltimore.
LaBarbera, M., 1984. Feeding currents and particle capture mechanisms in suspension feeding animals. Am. Zool. 24, 71–84.
Macy, W.K., Durbin, A.G., Durbin, E.G., 1999. Metabolic rate in relation to temperature and swimming speed, and the cost of filter feeding in Atlantic menhaden, *Brevoortia tyrannus*. Fish. Bull 97, 282–293.
Meekan, M.G., Jarman, S.N., McLean, C., Schultz, M.B., 2009. DNA evidence of whale sharks (*Rhincodon typus*) feeding on red crab (*Gecarcoidea natalis*) larvae at Christmas Island. Australia. Mar. Freshw. Res. 60, 607–609.
Mehta, R.D., Bradshaw, P., 1979. Design rules for small low speed wind tunnels. Aeronaut. J. Roy. Aeronaut. Soc. 73, 443–449.
Merino, M., 1997. Upwelling on the Yucatan shelf: hydrographic evidence. J. Mar. Sys. 13, 101–121.
Moin, P., Kim, J., 1985. The structure of the vorticity field in turbulent channel flow. Part I. Analysis of instantaneous fields and statistic correlations. J. Fluid Mech. 155, 441–464.
Motta, P.J., Wilga, C.D., 1999. Anatomy of the feeding apparatus of the nurse shark, *Ginglymostoma cirratum*. J. Morphol. 241, 1–29.
Mowbray, L.L., 1923. The taking of a whale shark (*Rhiniodon typus*) in Southern Florida. Bull. New York Zool. Soc. 26, 82–83.
Nakaya, K., Matsumoto, R., Suda, K., 2008. Feeding strategy of the megamouth shark *Megachasma pelagios* (Lamniformes: Megachasmidae). J. Fish Biol. 73, 17–34.
Nelson, J.D., Eckert, S.A., 2007. Foraging ecology of whale sharks (*Rhincodon typus*) within Bahia de Los Angeles, Baja California Norte. Mexico. Fish. Res 84, 47–64.
Pérez, R., Muller-Karger, F.E., Victoria, I., Melo, N., Cerdeira, S., 1999. Cuban, Mexican, U.S. researchers probing mysteries of Yucatan current. EOS Trans. AGU 80, 153–158.
Ripperger, S., Altmann, J., 2002. Crossflow microfiltration—state of the art. Sep. Purif. Technol. 26, 19–31.
Rowat, D., Gore, M., 2007. Regional scale horizontal and local scale vertical movements of whale sharks in the Indian Ocean off Seychelles. Fish. Res. 84, 32–40.
Rowat, D., Meekan, M.G., Engelhardt, U., Pardigon, B., Vely, M., 2007. Aggregations of juvenile whale sharks (*Rhincodon typus*) in the Gulf of Tadjoura. Djibouti. Environ. Biol. Fishes 80, 465–472.
Rowat, D., Gore, M., Meekan, M.G., Lawler, I.R., Bradshaw, C.J.A., 2009. Aerial survey as a tool to estimate whale shark abundance trends. J. Exp. Mar. Biol. Ecol. 368, 1–8.
Rubenstein, D.I., Koehl, M.A.R., 1977. The mechanisms of filter-feeding: some theoretical considerations. Am. Nat. 111, 981–994.
Sanderson, S.L., Wassersug, R., 1993. Convergent and alternative designs for vertebrate suspension feeding. In: Hanken, J., Hall, B.K. (Eds.), The Skull, vol. 3, Functional and Evolutionary Mechanisms. The University of Chicago Press, Chicago, pp. 37–112.
Sanderson, S.L., Cheer, A.Y., Goodrich, J.S., Graziano, J.D., Callan, W.T., 2001. Crossflow filtration in suspension-feeding fishes. Nature 412, 439–441.
Schmid, T.H., Murru, F.L., 1994. Bioenergetics of the bull shark, *Carcharhinus leucas*, maintained in captivity. Zoo Biol. 13, 177–185.
Schmidt, J.V., Schmidt, C.L., Ozer, F., Ernst, R.E., Feldheim, K.A., Ashley, M.V., Levine, M., 2009. Low genetic differentiation across three major ocean populations of the whale shark, *Rhincodon typus*. PLoS ONE 4, e4988, doi:10.1371/journal.pone.0004988.
Silas, E.G., Rajagopalan, M.S., 1963. On a recent capture of a whale shark (*Rhincodon typus* Smith) at Tuticorin, with a note on information to be obtained on whale sharks from Indian waters. J. Mar. Biol. Assoc. India 5, 153–157.
Simon, M., Johnson, M., Tyack, P., Madsen, P.T., 2009. Behaviour and kinematics of continuous ram filtration in bowhead whales (*Balaena mysticetus*). Proc. R. Soc. B 276, 3819–3828.
Sims, D.W., 1999. Threshold foraging behavior of basking sharks on zooplankton: life on an energetic knife-edge? Proc. R. Soc. Lond. B 266, 1437–1443.
Sims, D.W., 2000a. Can threshold foraging responses of basking sharks be used to estimate their metabolic rate? Mar. Ecol. Prog. Ser. 200, 289–296.
Sims, D.W., 2000b. Filter-feeding and cruising swimming speeds of basking sharks compared with optimal models: they filter-feed slower than predicted for their size. J. Exp. Mar. Biol. Ecol. 249, 65–76.
Sims, D.W., Merrett, D.A., 1997. Determination of zooplankton characteristics in the presence of surface feeding basking sharks *Cetorhinus maximus*. Mar. Ecol. Prog. Ser. 158, 297–302.
Sims, D.W., Quayle, V.A., 1998. Selective foraging behaviour of basking sharks on zooplankton in a small-scale front. Nature 393, 460–464.
Sims, D.W., Southall, E.J., Merrett, D.A., Sanders, J., 2003. Effects of zooplankton density and diel period on surface-swimming duration of basking sharks. J. Mar. Biol. Assoc. U. K. 83, 643–646.
Sims, D.W., Southall, E.J., Tarling, G.A., Metcalfe, J.D., 2005. Habitat-specific normal and reverse diel vertical migration in the plankton-feeding basking shark. J. Anim. Ecol. 74, 755–761.
Smith, A., 1829. Contributions to the natural history of South Africa. Zool. J. 16, 443–444.
Smith, A., 1849. Illustrations of the zoology of South Africa, vol. 4. In: Pisces. Smith, Elder and Co., London.
Smith, J.C., Sanderson, S.L., 2007. Mucus function and crossflow filtration in a fish with gill rakers removed versus intact. J. Exp. Biol. 210, 2706–2713.
Smith, J.C., Sanderson, S.L., 2008. Intra-oral flow patterns and speeds in a suspension-feeding fish with gill rakers removed versus intact. Biol. Bull. 215, 309–318.
Taylor, G., 1994. Whale Sharks, The Giants of Ningaloo Reef. Angus and Robertson, Sydney, Australia.
Taylor, J.G., 1996. Seasonal occurrence, distribution, and movements of the whale shark *Rhincodon typus*, at Ningaloo Reef, Western Australia. Mar. Freshw. Res 47, 637–642.
Taylor, J.G., 2007. Ram filter-feeding and nocturnal feeding of whale sharks (*Rhincodon typus*) at Ningaloo Reef, Western Australia. Fish. Res. 84, 65–70.
Taylor, J.G., Pearce, A.F., 1999. Ningaloo Reef currents: implications for coral spawn dispersal, zooplankton and whale shark abundance. J. R. Soc. West. Aust. 82, 57–65.
Taylor, L.R., Compagno, L.J.V., Struhsaker, P.J., 1983. Megamouth—a new species, genus, and family of lamnoid shark (*Megachasma pelagios*, family Megachasmidae) from the Hawaiian Islands. Proc. Calif. Acad. Sci. 43, 87–110.
Thurston, E., 1894. Inspection of Ceylon Pearl Banks. Bull. Madras Gov. Mus. 1, 36–38.
Tyminski, J., Hueter, R., de la Parra, R., 2008. The vertical movements of whale sharks tagged with pop-up archival satellite tags off Quintana Roo, Mexico. In: Proceedings of the 2nd International Whale Shark Conference, Holbox, Quintana Roo, Mexico, 15–20 July 2008, Available at: http://www.domino.conanp.gob.mx/doc_conf/John_T_Holbox_Vertical_Movements_Talk_Final.pdf.
Uchida, S., 1990. On the morphology of the whale shark, *Rhincodon typus* Smith. Okinawa Expo Aquarium. Collected Reprints 1976–1989 5, 165–173.
Videler, J.J., 1993. Fish Swimming. Chapman and Hall, London.
Ward-Smith, A.J., 1980. Internal Fluid Flow: The Fluid Dynamics of Flow in Pipes and Ducts. Oxford University Press, New York.
Weihs, D., 1977. Effects of size on sustained swimming speeds of aquatic organisms. In: Pedley, T.J. (Ed.), Scale Effects in Animal Locomotion. Academic Press, New York, pp. 333–338.
Weihs, D., Webb, P.W., 1983. Optimization of locomotion. In: Webb, P.W., Weihs, D. (Eds.), Fish Biomechanics. Praeger Publishers, New York, pp. 339–371.
Weihs, D., Keyes, R.S., Stalls, D.M., 1981. Voluntary swimming speeds of two species of large carcharhinid sharks. Copeia 1981, 219–222.
Werth, A.J., 2004. Models of hydrodynamic flow in the bowhead whale filter feeding apparatus. J. Exp. Biol. 207, 3569–3580.
Wetherbee, B.M., Cortes, E., 2004. Food consumption and feeding habits. In: Carrier, J.C., Musick, J.A., Heithaus, M.R. (Eds.), Biology of Sharks and Their Relatives. CRC Press, Boca Raton, pp. 225–246.
Wilga, C.D., Lauder, G.V., 2000. Three-dimensional kinematics and wake structure of the pectoral fins during locomotion in leopard sharks *Triakis semifasciata*. J. Exp. Biol. 203, 2261–2278.
Wilson, S.G., 2006. The biggest fish: unraveling the mysteries of the whale shark. Nat. Hist. 115, 42–47.
Wilson, S.G., Newbound, D.R., 2001. Two whale shark faecal samples from Ningaloo Reef, Western Australia. Bull. Mar. Sci. 68, 361–362.
Wilson, S.G., Taylor, J.G., Pearce, A.F., 2001. The seasonal aggregation of whale sharks at Ningaloo Reef, Western Australia: currents, migrations and the El Niño/Southern Oscillation. Environ. Biol. Fishes 61, 1–11.
Wilson, S.G., Polovina, J.J., Stewart, B.S., Meekan, M.G., 2006. Movements of whale sharks (*Rhincodon typus*) tagged at Ningaloo reef, Western Australia. Mar. Biol. 148, 1157–1166.
Zavala-Hidalgo, J., Gallegos-Garcia, A., Martinez-Lopez, B., Morey, S.L., O'Brien, J.J., 2006. Seasonal upwelling on the western and southern shelves of the Gulf of Mexico. Ocean Dyn. 56, 333–338.

Please cite this article in press as: Motta, P.J., et al., Feeding anatomy, filter-feeding rate, and diet of whale sharks *Rhincodon typus* during surface ram filter feeding off the Yucatan Peninsula, Mexico. Zoology (2010), doi:10.1016/j.zool.2009.12.001